Extreme Mechanics Letters 9 (2016) 97–107

Contents lists available at ScienceDirect

Extreme Mechanics Letters

journal homepage: www.elsevier.com/locate/eml

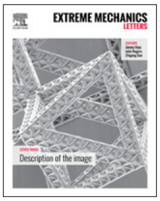

Towards prediction of the fatigue life of Ni microbeams under extreme stress gradients

F. Sadeghi-Tohidi, O.N. Pierron [*]

G.W. Woodruff School of Mechanical Engineering, Georgia Institute of Technology, Atlanta, GA, 30332-0405, USA

ARTICLE INFO

Article history:
Received 16 February 2016
Received in revised form 13 May 2016
Accepted 23 May 2016
Available online 2 June 2016

Keywords:
Fatigue life
Microstructurally small cracks
Electroplated Ni microbeams
Extreme stress gradients

ABSTRACT

This work investigated the effect of two extreme normalized stress gradients ($\eta = 17\%$ vs. 36% μm^{-1}) on the fully-reversed bending fatigue behavior (fatigue life and fatigue crack propagation curves) of 20-μm-thick, electroplated Ni microbeams, in humid air environments. The results highlight the significant challenge in predicting the bending fatigue life of microbeams subjected to extreme stress gradients, which was measured to be three order of magnitudes larger for $\eta = 36\%\ \mu\text{m}^{-1}$ at a stress amplitude of ∼450 MPa. The fatigue life is dominated by the ultraslow growth of microstructurally small cracks, which is a strong function of the normalized stress gradient. For $\eta = 17\%\ \mu\text{m}^{-1}$, the crack growth rates are initially about one order of magnitude larger than for $\eta = 36\%\ \mu\text{m}^{-1}$ and, in contrast to the larger stress gradient microbeams, do not decrease with increasing crack size. This singular behavior results in low Basquin and Coffin–Manson exponents (in absolute value) compared to $\eta = 0$. As a result, the fatigue endurance limit increases from 35% to 50% of the tensile strength for η increasing from 17% to 36% μm^{-1}, compared to 30% in the absence of stress gradients. The environmental effects are also discussed.

1. Introduction

Fatigue degradation in bulk structures usually occurs first ahead of notches, at the location of stress concentrations. The fatigue limit of a notched structure, in term of notch root stress ($\sigma_{\text{e,n}}$), is typically larger than that of a smooth specimen ($S_{\text{e,u}}$): $\sigma_{\text{e,n}} > S_{\text{e,u}}$. In term of nominal, far-field stress, the fatigue limit of a notched structure ($S_{\text{e,n}}$) is larger than the unnotched limit divided by the stress concentration factor, k_t: $S_{\text{e,n}} > S_{\text{e,u}}/k_t$. The ratio between unnotched and notched limit is defined as the fatigue notch factor, $k_f = S_{\text{e,u}}/S_{\text{e,n}}$. The physical explanation is related to the stress gradients that are present ahead of a notch and the fact that fatigue occurs within a process zone of a finite volume that is subjected to a lower average stress than the maximum stress at the notch root [1]. The prediction of the notched fatigue limit from the known unnotched fatigue limit (or equivalently the prediction of k_f) requires an empirical equation of the notch sensitivity factor, q, defined as

$$q = \frac{k_f - 1}{k_t - 1}. \quad (1)$$

The empirical equations for q depend on the material and notch root radius, such as the Peterson equation [1]:

$$q = \frac{1}{1 + \frac{\alpha}{\rho}} \quad (2)$$

with α being a material constant and ρ the notch radius. This empirical equation captures the experimental trend that the sharper the notch, the larger the notch root stress fatigue limit, due to the larger stress gradients. The effects of stress gradients were more directly taken into account by Lukas and Klesnil who developed a model to predict fatigue limits in notched bodies that relies on the stress

---

[*] Corresponding author. Tel.: +1 404 894 777.
E-mail address: olivier.pierron@me.gatech.edu (O.N. Pierron).

http://dx.doi.org/10.1016/j.eml.2016.05.011
2352-4316/

intensity factor formulas ahead of notches and on the fact that fatigue failure occurs if a crack can grow large enough to reach a critical size that corresponds to the threshold stress intensity factor range, ΔKth (for long cracks) [2]. One additional reason for the sharp notch increased fatigue limit is the formation of non-propagating cracks—cracks nucleating at the notch root but unable to propagate due to the decreasing stress intensity factor range with increasing crack size, which occurs for sharp enough notches (for example, less than 2.5 mm for circular notches) [3,4].

It is important to realize that the aforementioned approaches to predict the fatigue limit of notched components in bulk materials cannot necessarily be applied to microscale equivalents, such as metallic microbeams under bending. In these micro-components (especially under bending), the stress gradients are much steeper than in bulk materials due to the microscopic dimensions. Typical normalized stress gradients, η, defined as:

$$\eta = \frac{1}{\sigma_{\max}} \frac{d\sigma}{dx} \qquad (3)$$

where $d\sigma/dx$ represents the stress gradient across the beam (with or without the presence of a notch for bending loading), do not exceed 1%–2% μm^{-1} in bulk materials [2,5]. In contrast, η can be more than one order of magnitude larger for microbeams under bending, making the investigation of this *physical* size effect an outstanding challenge to accurately predict the bending fatigue life of metallic micro-components widely used in applications such as flexible/stretchable electronics and micro/nano electromechanical systems (MEMS/NEMS) [6–12]. In addition, another *microstructural* size effect must be considered as well, related to the fact that fatigue cracks propagating from the edges of microbeams towards the neutral axis are microstructurally small (their size is commensurate with the grain size), and therefore do not follow the classical crack propagation equations (Paris law) [13]. We recently highlighted the singular fatigue behavior of electroplated Ni notched microbeams with normalized stress gradients of 36% μm^{-1}, characterized by a large endurance limit (50% of the ultimate tensile strength, vs. 30% for bulk Ni or electroplated Ni films under tensile loading) and "shallow" stress–life and strain–life curves [14]. This singular behavior appeared to result from the growth of microstructurally small cracks under extreme stress gradients which was characterized as ultraslow with decelerating crack growth rates. That study highlighted the need to further characterize the effects of different stress gradients values on crack growth rates and fatigue lives in order to accurately predict the small-scale fatigue damage in metallic microbeams. In this paper, we compare the fully-reversed bending fatigue behavior of electroplated Ni microbeams with two different geometries, corresponding to two different η (17 vs. 36% μm^{-1}) in order to unambiguously determine the extreme stress gradient effects in small-scale fatigue.

2. Methods

The principle of operation of the Ni fatigue microresonators used in this study has already been described in details in previous publications [14–18]; hence only a brief description of the method is given in this section, with a focus on the difference in microbeam geometry which results in different η values.

2.1. Fatigue specimens and material

Fig. 1(a) shows a SEM image of a Ni microresonator, while Fig. 1(b) and (c) shows images of the two microbeam geometries employed in this study. These specimens were fabricated with the Metal MUMPs process from MEMSCAP. Metal MUMPs is an electroplated Ni micromachining process, which includes the patterning of a thick layer of photoresist that forms a patterned stencil for the electroplated Ni. The electroplating process is at 30 °C, with a current density of 20 mA/cm^2 and a pH level of 4 [19]. The notched microbeam (see Fig. 1(c)) is 14.8 μm wide with a 4-μm-root-radius notch, corresponding to $\eta = 36\%\ \mu\text{m}^{-1}$ over the first two micrometers (see stress profile across the beam's width in Fig. 1(e) and below for details). The other microbeam (see Fig. 1(b)) has a width of 11.3 μm at its narrowest section, which corresponds to $\eta = 17\%\ \mu\text{m}^{-1}$ (see stress profile across its width in Fig. 1(d) and below for details). Both microbeams are 20 μm thick, with a 0.5-μm-thick Au layer on top, and are connected to a large fan-shaped mass with two sets of interdigitated fingers (two "combs", one for electrostatic actuation and one for capacitive sensing of motion); see Fig. 1(a).

The tensile properties of the 20-μm-thick electroplated Ni layer have already been measured: yield stress of 656 ± 70 MPa, tensile strength of 873 ± 26 MPa, and ductility of 7.4 ± 2.8% [16]; see Table S1 in the Supplementary Information giving also the fitting parameters for the Ramberg–Osgood constitutive equation, from which the stress–strain curve shown in Fig. 1(f) was obtained. The Ni layer has a strong $\langle 001\rangle$ crystallographic out-of-plane texture and a columnar microstructure, with columnar grains that are ∼5–10 μm in height and ∼1–2 μm in width [16]. The elastic modulus ($E_{\text{Ni}} = 172$ GPa at 30 °C, and 166 GPa at 80 °C) used in this study is consistent with this texture [16]. The cross-section of the microbeams at the location of fatigue damage for both geometries therefore consists of ∼5–10 grains across the width and ∼2–4 grains across the thickness. Although there is a limited number of grains through the specimen's width, the stress gradients were calculated using finite element models with the material properties listed in Table S1. The low variability in the measured initial f_0 between specimens (see Section 3.1) and the good match between the measured f_0 and the calculated one from finite element modal analysis [16] justify the use of this model to characterize the stress gradients.

2.2. Fatigue testing principles

The microresonators consist of a micro-scale equivalent of bulk ultrasonic fatigue testers: driven at resonance (resonance frequency, $f_0 \sim 8$–10 kHz), they lead to fully-reversed cyclic bending of the microbeams, and fatigue failure under large enough amplitudes of rotation [14,20]. During a fatigue test (performed in controlled environments, either mild (30 °C, 50% RH), or harsh (80 °C, 90%